Derivation of Yield Function Constants for Modeling the PM-Compaction

Chidanand. G, Sachin,B.M., Thilak B.T., Shashidhar, U.G.,Shamasundar S.
ProSIM R&D Center,
21/B, 9th Main, Shankara Nagara, Mahalakshmi Puram Bangalore 560096
Tel /fax: 080 2357 8292 email: info@pro-sim.com

ABSTRACT

Triaxial tests have been used to derive the yield function and constitutive equations of the powder mass undergoing compaction. The spring back due to elastic recovery of the green is an industrially important parameter which has received very little effort in modeling. The set of experiments conducted included the careful consideration of strain paths to study the elastic behavior during compaction. The bulk modulii, elastic modulii dilation angle and other parameters were derived by experiments. These parameters form a vital component in the FEM analysis of compaction process.

Care to be taken in the design of the experiments, need for proper analysis of the experimental data, methodology for derivation of the constants is described in the paper.

Keywords: Powder Metallurgy Compaction, Yield Criteria, Triaxial Test.

1. Introduction

The compaction of powders to form both bulk materials and net-shaped parts has become a successful and well-established process for metals, alloys, polymers and ceramics. In the powder metallurgy (PM) industry a popular process route is cold compaction by rate-independent plasticity, followed by pressure-less sintering by diffusion flow. In hot pressing, compaction is by power law creep and/or diffusion flow. Although significant empirical progress has been made to optimize compaction procedures with respect to pressure, temperature and time, a concise and general micromechanical model, free from phenomenological assumptions, has been lacking. Early constitutive descriptions have been empirical in nature, with no underlying modeling (see for example, Kuhn and Downey, 1971; Shima and Oyane, 1976). Herein, a micromechanical model is developed for powder compaction by both plasticity and power-law creep, with the relative density in the practical range of 0.6-0.8. The essential physics are the relationship between the macroscopic strain and the local kinematics of particle contact, and the relationship between local contact loads and the resulting macroscopic stress. The model is appropriate for the so-called Stage 1 regime, with relative density of the compact approximately in the range 0.6-0.8.

The die compaction of powders has been used in manufacturing components for a broad range of applications. In engineering applications, the green compact of uniform density is a fundamental requirement for the production of a good quality and high strength part. Density inhomogeneity can be caused by friction force owing to interparticle movement and relative slip between the powder particles and the die wall. Also, the die geometry and the sequence of punch movement's results in a lack of density homogeneity for a compact of complex shape. Therefore, creating the right tooling design is very important for the success of powder compaction processes.

Generally, the design can be achieved by an empirical approach or a computer aided approach. A computer aided approach offers the designer a computational tool to reduce time and cost for process development, using an appropriate mathematical model to simulate and investigate the compaction process without actually constructing the system. For the computer aided approach, several mathematical models for porous material have been proposed.[1–5] Lee and Kim[4] modified a yield criterion for porous material which was suggested by Doraivelu et al.[3] and could incorporate one empirical parameter that can be estimated from the yield stress v. initial relative density data. Using the yield criterion, Han et al.[5] formulated an elasto-plastic finite element code and analyzed the deformation of sintered metals in simple upsetting, indenting, ring compression, and hot forging.[7] Also, Han et al.[8] calculated the forging limit curves of sintered porous metals with the Lee–Kuhn initial imperfection model.[9]

In the case of powder compaction at room temperature, the manner of densification differs from that of sintered porous material. In cold compaction, the densification of a powder compact can be classified into two stages.[10–12] In the first stage, where the arrangement of powder particles changes, powder particles rearrange by sliding and local plastic deformation or fracture at surface irregularities.[12] In the second stage where the relative motion among powder particles is small or negligible, the manner of densification becomes similar to that of sintered porous material.

The shape and initial porosity of powder particles are important material characteristics at the first stage, where sliding and local plastic deformation or fracture plays an important role. Generally, at the initial stage of compaction, the powder compact of high porosity or irregular shape shows low apparent relative density and can be densified more easily than the compact of low porosity or spherical shape. Thus, the effects of particle shape or porosity have to be taken into account in the yield criterion to simulate overall powder compaction. Park et al.[13] modified the yield criterion suggested by Lee and Kim,[4] so that the modified yield criterion could successfully incorporate empirical parameters which reflect the characteristics of copper powders of different particle shape during uniaxial compaction.

In the case of ceramic powders, it is not certain that the yield criterion proposed by Park et al.[13] could be used in analysis of compaction or other densification processes, because ceramic powders have no plasticity. In the present paper, the densification behavior of ceramic powders is analyzed using the yield criterion suggested by Park et al.[13] The relation between parameters in the yield criterion and morphological and mechanical

characteristics of ceramic powders is investigated. Also, the elasto-plastic finite element calculation is carried out to simulate the uniaxial compaction process of ceramic powders.

2. Yield criteria

Recall that we say that the material yields when it exhibits an irreversible straining which is sustained once a certain level of the stress distribution is reached. A yield criterion indicates for which combination of stress components transition from elastic (recoverable) to plastic (permanent) deformations occurs.

We will start our discussion with initial yielding and then proceed to discuss how material yielding is sustained. In one-dimension (Figure.1 (a)) yielding occurs when the uniaxial stress reaches the value of the yield stress Y in tension, i.e. at $\sigma = Y$. When does 'yielding' occurs in multi-axial stress states? (Figure.1 (b))? The answer is given with phenomenological theories called 'yield criteria'. Instead of presenting the requirements and constraints for a general form of a yield criterion, we will here only examine the two most important yield criteria for isotropic materials.

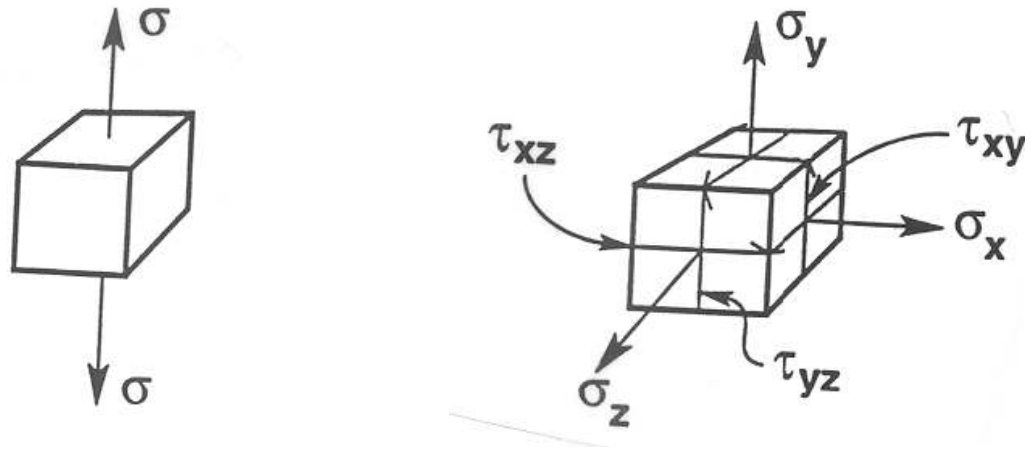

Figure 1: (a) To define yielding in one-dimensional stress states, we compare the uniaxial stress σ with the yield stress in tension Y. (b) When does yielding occurs in multi-dimensions?

3. Constitutive models

Constitutive models for the continuum, which include elasticity and several plasticity models like Mohr-Coulomb, Von Misès and Drucker-Prager, the last one coupled with a cap-closure, essential for nonlinear consolidation. A large variety of soils, and even concrete, can be adequately represented by these models. A tension cut-off for materials with limited tensile resistance is also included in most models.
In addition, new developments include a multilaminate model for layered media, Rankine plasticity and a Hoek-Brown type yield surface.

3.1 Plasticity

The basic plastic models, i.e. Mohr-Coulomb and Drucker-Prager require only the elastic constants E (Young's modulus), ν (Poisson's ratio), the cohesion C and friction angle ϕ.

3.1.1 Mohr-Coulomb criterion (M-C)

The Mohr-Coulomb surface is defined by two-constant C and ϕ. The equation of the criterion in two dimensional stress space is

$$\tau = C + \sigma \tan\phi \tag{3.1}$$

The corresponding surface in three-dimensional stress space is characterized by a cone with vertices in the deviatoric cross section. For convenience this surface is replaced by a smooth surface illustrated in Figure 2 [MEN, 1995][21] and defined by equations (3.2)

$$f = \frac{1}{2}(3 - \sin\phi)\rho r(\theta, e) + \sqrt{2}\sin\phi\xi - \sqrt{6c}\cos\phi \tag{3.2.a}$$

with

$$r(\theta, e) = \frac{4(1-e^2)\cos^2\theta + (2e-1)^2}{2(1-e^2)\cos\theta + (2e-1)\left[4(1-e^2)\cos^2\theta + 5e^2 - 4e\right]^{1/2}} \tag{3.2.b}$$

$$e = \frac{3-\sin\phi}{3+\sin\phi} \quad (3.2.c) \qquad \rho = \sqrt{2J_2} \quad (3.2.d) \qquad \xi = \frac{1}{\sqrt{3I_1}} \quad (3.2.e)$$

and I_1 and J_2 are the fundamental stress invariants.

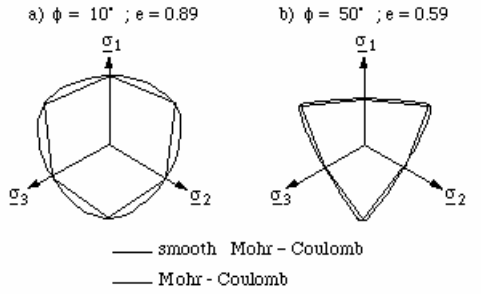

Figure 2 - Smooth Mohr-Coulomb surface [MEN, 1995] [21]

The plastic flow direction is an essential component of the plastic model. The most appropriate flow also may depend on the type of analysis (deformation or ultimate load). Default options are provided to help the user, which for ultimate load analysis will lead to a crisp and reliable capture of failure mechanisms.

3.1.2 Drucker-Prager criterion (D-P)

The Drucker-Prager criterion (Equation 3.3) is more convenient from the point of view of numerical efficiency, it is therefore often preferred to the Mohr-Coulomb criterion.
From the comparison of both D-P and M-C criteria it is obvious that different size adjustments are possible which correspond to different matching of the Mohr-Coulomb parameters C and ϕ with the Drucker-Prager parameters a and k, and this selection obviously affects the yield stress (Figure. 3)

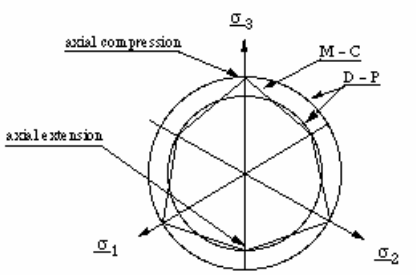

Figure 3 - Deviatoric section of Mohr-Coulomb criterion and Drucker-Prager with two different size adjustments

$$f(\sigma) = aI_1 + \sqrt{J_2} - k = 0 \qquad (3.3)$$

I_1 and J_2 are stress invariants and constants a, k can be defined from common geotechnical data: cohesion C and angle of friction ϕ;

$$\left.\begin{aligned} a &= \sin\frac{\phi}{3} \\ k &= C\cos\phi \end{aligned}\right\} \quad \text{for plane strain and deviatoric flow} \qquad (3.3.a)$$

$$\left.\begin{aligned} a &= \left(2\sqrt{3}\sin\phi \big/ (9 - \sin^2\phi)\right) \\ k &= \left(6\sqrt{3}C\cos\phi \big/ (9 - \sin^2\phi)\right) \end{aligned}\right\} \quad \text{for axisymmetry} \qquad (3.3.b)$$

The plane strain adjustment corresponds to an adjustment of failure loads.

Cap model

A cap model coupled to the Drucker-Prager criterion is provided for the simulation of nonlinear consolidation. The model requires three additional data from an oedometer test: the initial void ratio e_0, the vertical stress at yield and λ the compression index which characterizes plastic hardening (Figure 4).

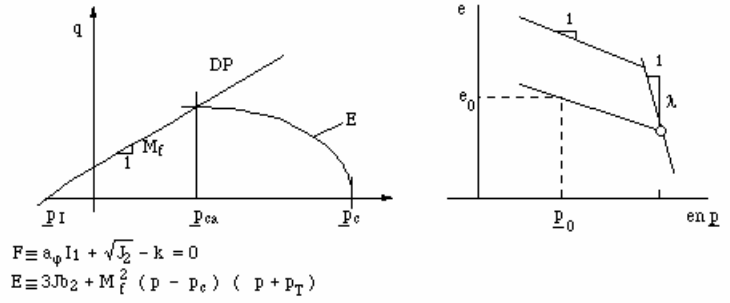

Figure 4.a - Drucker-Prager Model with cap closure Figure 4.b - Oedometer test

3.1.3 Multilaminate model

One to three weakness planes orientations can be introduced which will remain fixed in space. Each is characterized by a cohesion c^i, a friction angle and a dilatancy (non-associative angle ψ^i). A tensile cut-off can be specified with f_t^i the maximum tensile stress.

On each plane separately, the Mohr-Coulomb plasticity condition and the tension cut-off condition must be fulfilled.

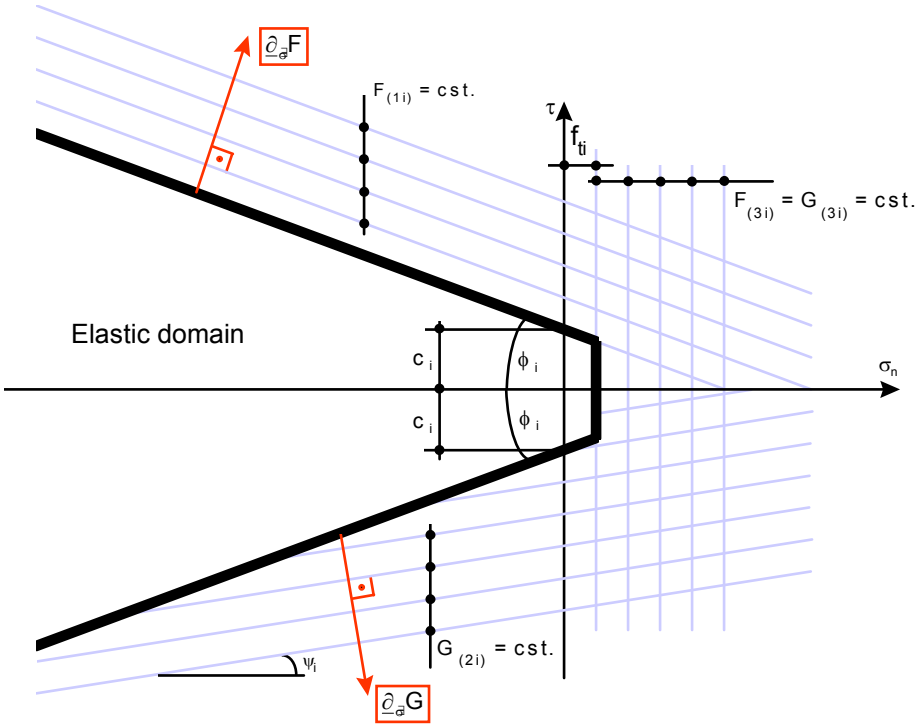

Figure 5 - Weakness plane plasticity conditions, yield function and flow potential isolines

Plasticity and flow rule conditions can be derived for each plane i=1, ..., 3 :

$$F^{(1i)} = \tau + \sigma_n \mathrm{tg}\phi^i - c^i$$

$$F^{(2i)} = -\tau + \sigma_n \mathrm{tg}\phi^i - c^i$$

$$F^{(3i)} = \sigma_n - f_t$$

4. Experimental Procedure:

4.1 Index properties

4.1.1 Specific gravity: Specific gravity of the powder is determined as per IS: 2720- Part 3 (1980). The specific gravity of the powder is obtained as 7.18.

4.1.2 Grain size distribution: The grain size distribution of the powder is determined from sieve analysis conducted as per IS: 2720- Part 4 (1985). The powder has 65% of the particles passing through 75 μ sieve and 35% of the particles retained on 75 μ sieve (passing 300 μ sieve). The average size of the particle is close to the size of fine grained silty sand.

4.1.3 Maximum and Minimum dry densities: The minimum dry density of the powder is obtained by loosely pouring the powder into a cylinder of known volume. Maximum

dry density under no compressive load is obtained by vibrating the powder in a vibrating table for 8 mins. The values of minimum and maximum dry densities obtained are 3.7 and 4.4 g/cc respectively.

4.2 Shear Strength Properties

The triaxial compression test is used to determine stress-strain properties and shear strength parameters of the powder. The test is conducted according to IS:2720- Part 11 (1971). The schematic diagram of the test set-up used is shown in Figure 6.

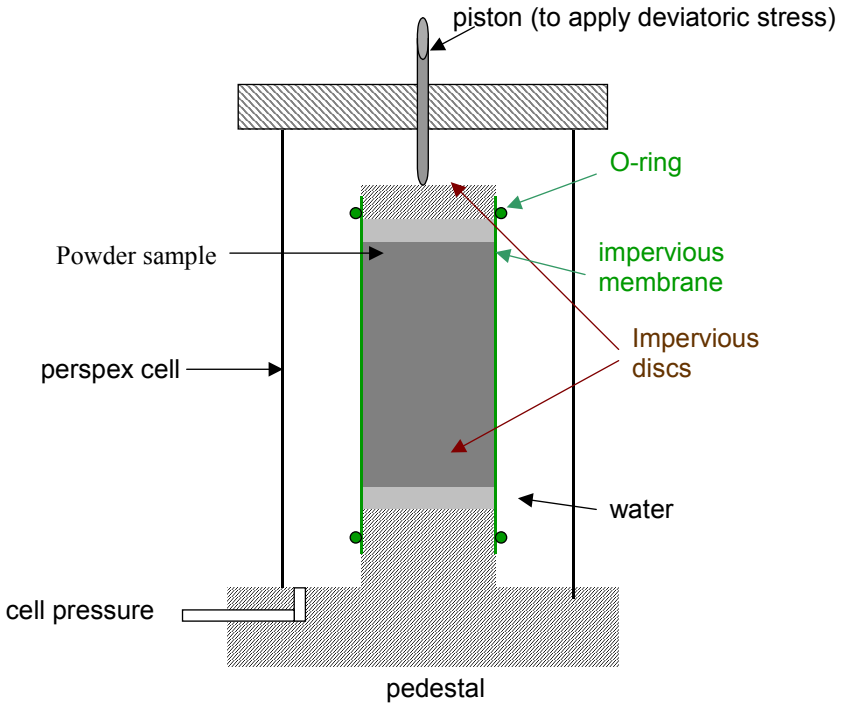

Figure 6. Triaxial compression test set-up

Cylindrical sample of the powder is prepared at a density of 3.7 g/cc for the triaxial test. The sample is 38 mm in diameter and from 76 mm in length. Four tests were carried out at four different confining pressures (50, 100, 200 and 300 kPa) on four identical samples (prepared to same density).

Results from Triaxial Tests

The strain and corresponding stress of the sample is plotted with stress abscissa and stress-strain curve for the powder is drawn. The maximum compressive stress at failure and the corresponding strain and cell pressure are found out. The stress-strain curves of the samples obtained from triaxial compression tests at different confining pressures are given in Figure 7. The Mean p vs. q plot for the powder is shown in Figure 8. The failure envelope joining the peaks of p-q plot is also shown in the Figure 8.

$$\text{Mean } p = (\sigma_1 + 2\,\sigma_3)/3; \qquad q = (\sigma_1 - \sigma_3)/2$$

From the slope of p-q line the angle of internal friction (ϕ) of the powder is obtained as 45^0. The powder is cohesionless as the p-q line has no y-intercept. The failure envelope is nonlinear at higher mean pressures.

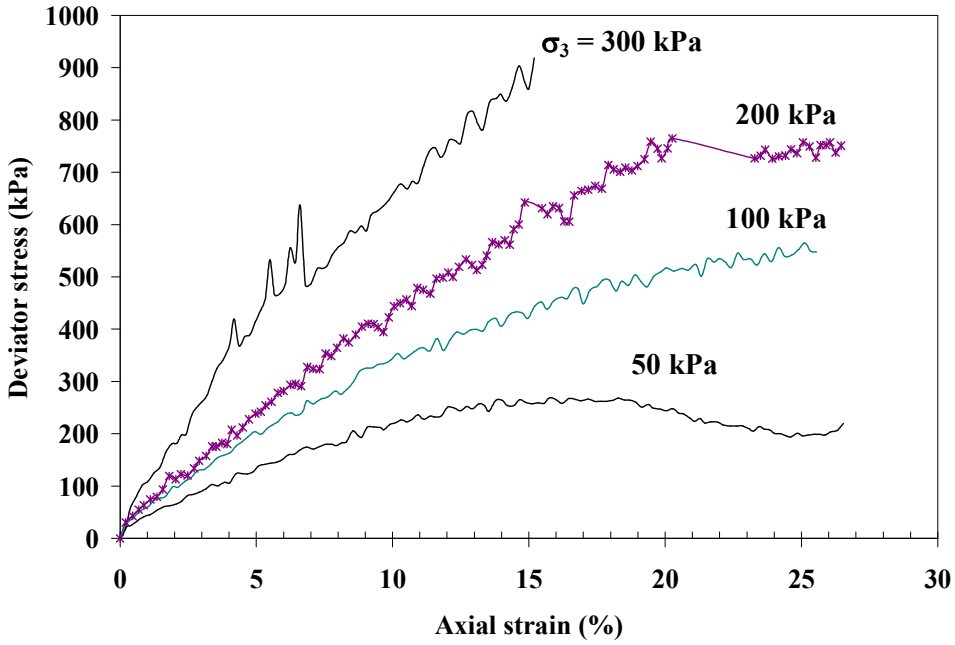

Figure 7. Stress-strain curves for the powder obtained from triaxial compression test

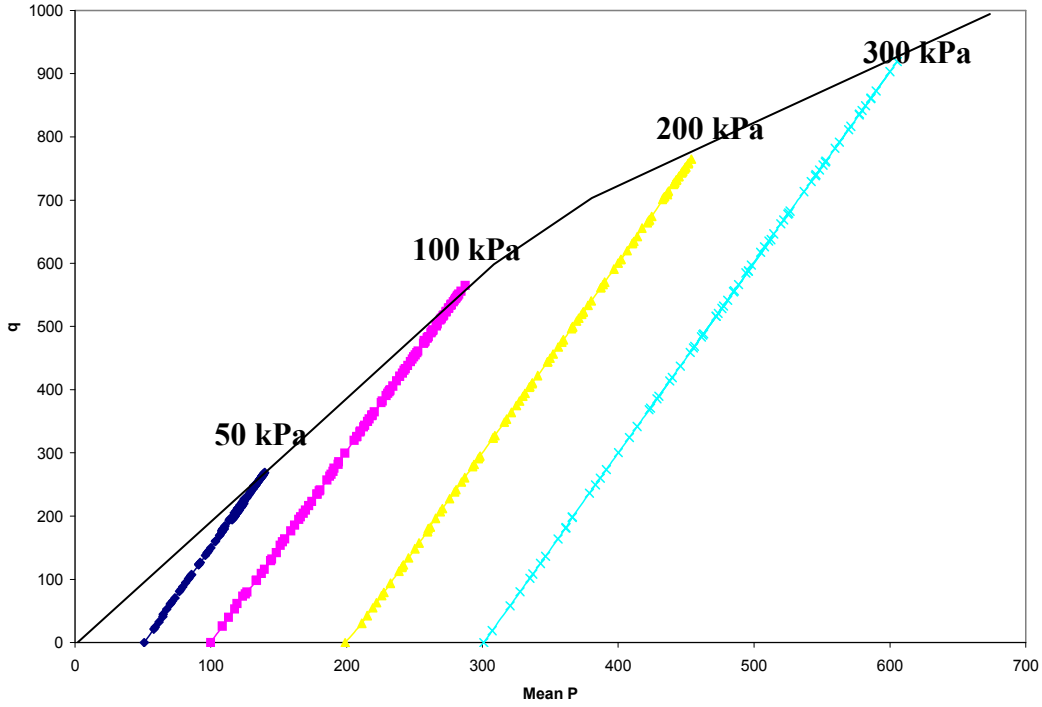

Figure 8. Mean p vs q diagram for the powder

4.3 Compression Properties

One dimensional compression test was carried out on powder in oedometer to determine the deformations in sample under uniaxial one-dimensional compression.

Procedure: Oedometer essentially consists of a steel ring of diameter 60mm and height 20mm in which the sample is prepared, loading device and dial gauge. Loading device consisting of frame, lever system, loading yoke dial gauge fixing device and weights. The powder is poured into the oedometer ring in loosest density. Initial load of 0.05 kg/cm^2 is applied to the powder sample placed between two end platens and allowed to stand until there is no change in dial gauge readings for two consecutive hours or for a maximum of 24 hours. Final dial reading under the initial load is noted. First load of intensity 0.1 kg/cm^2 is applied and dial gauge readings are recorded at various time intervals until there is no change in dial gauge reading for 30 minutes. Then the load intensity is doubled and the deformations are measured at time intervals. This procedure is repeated for successive load increments. The loading intensities applied are: 0.1, 0.2, 0.5, 1, 2, 4 and 8 kg/cm^2. After the last loading is completed, the load is reduced to ¼th of the value of the last load and allowed to stand for 1 hr. Then the load is reduced further in steps of ¼th the previous intensity till an intensity of 0.1 kg/cm^2 is reached. Final reading of the dial gauge is noted.

***Load-deformation Curve*:** The load deformation curve for the powder obtained from the one-dimensional compression test is shown in Figure 9.

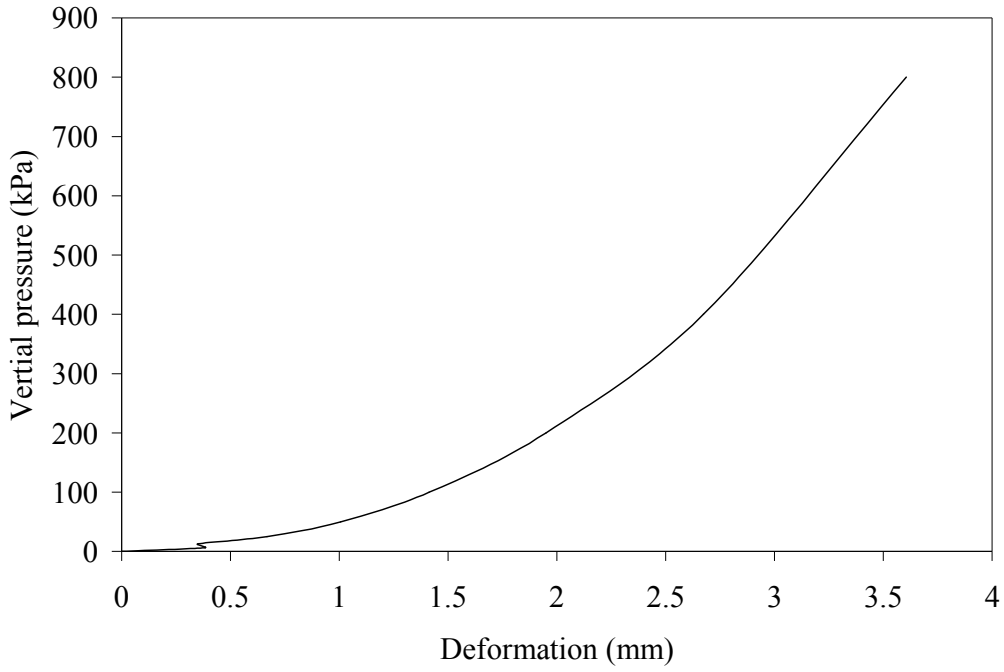

Figure 9. Load-deformation curve from One-dimensional compression test

5. Conclusion

The aim of this work was to Derivation of Yield Function for Modeling of PM-Compaction using the triaxial test data which has been developed by the oedometer under uniaxial one-dimensional compression. For developing a methodology for predicting the green density distribution using numerical simulations of powder compaction and of the ejection of the part from the die. This would enable sinter metal, hard metal, and ceramic part producers to optimize the tools and the press kinematics in the computer, before the tool is manufactured and tested, or to detect weaknesses in existing processes. The simpler part of this task is the prediction of the green density distribution.

REFERENCES

1. S. SHIMA and M. OYANE: Int. J. Mech. Sci., 1976, 18, 285–291.
2. L. GURSON: J. Eng. Mater. Technol. (T rans. ASME), 1977, 99, 2–15.
3. S. M. DORAIVELU, H. L. GEGEL, J. S. GUNASEKERA, J. C. MALAS, J. T. MORGAN, and J. F. THOMAS, Jr: Int. J. Mech. Sci., 1984, 26, 527–535.
4. D. N. LEE and H. S. KIM: Powder Metall., 1992, 35, 275–279.
5. H. N. HAN, H. S. KIM, K. H. OH, and D. N. LEE: Powder Metall., 1994, 37, 140–146.
6. H. N. HAN, H. S. KIM, K. H. OH, and D. N. LEE: Powder Metall., 1994, 37, 259–264.
7. H. N. HAN, Y. LEE, K. H. OH, and D. N. LEE: Mater. Sci. Eng. A, 1996, 206, 81–89.
8. H. N. HAN, K. H. OH, and D. N. LEE: Scr. Metall. Mater., 1995, 32, 1937–1944.
9. P. W. LEE and H. A. KUHN: Metall. T rans., 1973, 4, 969–974.
10. H. F. FISCHMEISTER, E. ARZT, and L. R. OLSSON: Powder Metall., 1978, 21, 179–187.
11. R. L. HEWITT, W. WALLACE, and M. C. DE MALHERBE: Powder Metall., 1974, 17, 1–12.
12. P. J. JAMES: Powder Metall., 1977, 20, 199–204.
13. S.-J. PARK, H. N. HAN, K. H. OH, and D. N. LEE: Int. J. Mech. Sci., 1999, 41, 121–141.
14. B. BUDIANSKY: J. Comp. Mater., 1970, 4, 286–295.
15. M. M. GAUTHIER: 'Engineered materials handbook', 103; 1995, Materials Park, OH, ASM International.
16. [BOW, 1979] - Bowles J.E. Physical and geotechnical properties of soils, p. 323.
17. [CHE, 1975] - Limit analysis and soil plasticity. Elsevier.
18. [CHE, 1982] - Plasticity in reinforced concrete. Mc Graw Hill.
19. [CHE, 1990] - Chen W.F., Liu W.K. Limit analysis in soil mechanics. Elsevier.
20. [COX, 1961] - Cox A.D., Eason G., and Hopkins H.G. Axially symmetric plastic deformation in soils. Philosophical transactions of the royal society of London, 254, 1-45.
21. [MEN, 1995] - Menétrey Ph., Willam K. A triaxial failure criterion for concrete and its generalization. ACI Journal 92 (3), pp. 311.318.
22. [SCH, 1969] - Schiffmann R.L., Chen A.T., Jordan J.C. An analysis of consolidation theories. J. of the Soil Mechanics & Foundations Div., vol. 95, No 1, pp. 285-312.
23. [TRU, 1997b] - Truty A., Zimmermann Th., Commend S., Urbanski A., Li Y. Numerical simulation of stability and failure in elasto-plastic layered media. Trans. IACMAG, Wuhan, China, 1997.
24. ABAQUS Analysis User's Manual Volume-III:Materials, Ver. 6.5, HKS Inc., 2005, P. 317-339.
25. ABAQUS Theory Manual, Ver. 6.5, HKS Inc., 2005, P. 115.